bioRxiv preprint doi: https://doi.org/10.1101/527572; this version posted January 22, 2019. The copyright holder for this preprint (which was not certified by peer review) is the author/funder. All rights reserved. No reuse allowed without permission.

Title: C99, not beta-amyloid, is associated with selective death of vulnerable neurons in Alzheimer's disease.

Authors: Maria Pulina[1], Maya Hopkins[1], Vahram Haroutunian[2], Paul Greengard[1], and Victor Bustos[1*]

Affiliations:

[1] Laboratory of Molecular and Cellular Neuroscience, The Rockefeller University, New York, NY 10065, USA.

[2] Icahn School of Medicine at Mount Sinai, NY and JJ Peters VA Medical Center, Bronx NY.

*Correspondence to: vbustos@rockefeller.edu

Abstract: Amyloid Precursor Protein (APP) and its cleavage product beta-amyloid are widely believed to be key players in the development of Alzheimer's disease (AD). However, the distribution of amyloid deposits in the brain does not correlate well with disease progression. Therefore, it seemed possible that APP metabolites other than beta-amyloid might make a strong contribution to AD pathology. We developed a sensitive assay adapted to the detection of C99, an intermediate in the conversion of APP to beta-amyloid. Brain tissue sections were obtained from patients suffering from sporadic AD and non-demented controls. Our results demonstrate that C99 levels, but not Abeta levels, correlate with the degree of vulnerability to neurodegeneration and cognitive impairment in patients suffering from AD.

bioRxiv preprint doi: https://doi.org/10.1101/527572; this version posted January 22, 2019. The copyright holder for this preprint (which was not certified by peer review) is the author/funder. All rights reserved. No reuse allowed without permission.

Main Text: Alzheimer's disease (AD) is the most common type of dementia, characterized by accumulation of extracellular and intracellular beta-amyloid aggregates, intracellular paired helical fragments and extensive age-dependent neuronal loss in vulnerable areas (*1-3*). Robust genetic and biochemical evidence points to alterations of APP metabolism as causative in the development of Alzheimer's disease. In the amyloidogenic pathway, APP is cleaved by beta-secretase (BACE) to generate sAPPb and C99. Gamma-secretase then cleaves C99 to generate beta-amyloid and AICD. Accumulation of beta-amyloid is a cardinal feature of Alzheimer's disease, but its role in causing injury in AD remains unclear. Thus, the distribution of beta-amyloid deposits in AD brains has a poor correlation with dementia severity, loss of neural function and cognitive impairment (*4-8*). Therefore, it is possible that APP metabolites other than beta-amyloid make a significant contribution to AD pathophysiology. In addressing this issue, a challenge has been the inability to determine the distribution and levels of specific APP metabolites in intact cells and tissues. We have approached this problem by adapting the proximity ligation assay (PLA) for the detection of C99. In this assay, two primary antibodies recognize the target epitopes on the protein of interest. If the epitopes are in close proximity, secondary antibodies covalently bound to complementary DNA strands participate in rolling circle DNA synthesis. The DNA synthesis reaction results in a one thousand-fold amplification of the DNA circle. Fluorescently-labeled complementary oligonucleotide probes added to the reaction bind to the amplified DNA. The resulting fluorescent signal can be detected by fluorescence microscopy. This technique offers great sensitivity, since powerful rolling circle amplification is used. It also offers great selectivity, since dual target recognition is used (*9*). Here, we used antibodies generated against both the N and C terminal domains of C99 in cultured cells and found that we can distinguish C99 from beta-amyloid, full-length APP, C83, and AICD. The adaptation of the proximity ligation assay to the detection of C99 provides a general framework for the detection *in situ* of low-abundance proteolytic fragments in human brain and animal models.

In a first step, we screened several antibodies aimed at recognizing the N and C-terminal domains of C99. The combination of 6C3, a mouse monoclonal antibody (*10*) which recognizes the cleaved N-terminal of C99 and RU-369, a rabbit polyclonal antibody (*11*) designed to recognize the C-terminal of APP, successfully recognizes C99 (**Figure 1A**). As expected with a C99-specific marker, the signal was greatly reduced by a BACE inhibitor, which blocks C99 synthesis, and dramatically increased by a gamma-secretase inhibitor, which blocks C99 breakdown (**Figure 1B**).

bioRxiv preprint doi: https://doi.org/10.1101/527572; this version posted January 22, 2019. The copyright holder for this preprint (which was not certified by peer review) is the author/funder. All rights reserved. No reuse allowed without permission.

C99-PLA produces bright red dots that can easily be quantified. Super-resolution microscopy reveals that each dot, measuring about 200-400 nm, consists of a group of 2-3 smaller dots, consistent with the idea of aggregation of C99 molecules (**Figure 1C**).

Next, we applied this PLA methodology to study the localization of C99 in human brain tissue. Brain tissue sections were obtained from hippocampus, frontal cortex and occipital cortex from 12 controls and 38 patients suffering from sporadic Alzheimer's disease. Age at the time of death and sex of these subjects is listed in Supplementary Table 1. PLA specificity was verified by omitting one of the antibodies (Supplementary figure 1). As seen in **Figure 2A**, C99 is readily detected in the soma and processes of neurons of cognitively normal patients.

To investigate whether C99 levels correlate with cognitive decline, three postmortem groups were studied: subjects with normal and stable cognition, as measured by the clinical dementia rating (CDR = 0), subjects with moderate AD (CDR = 0.5-2), and subjects with severe AD (CDR = 3-5). Average C99 levels were increased in the CA1 area of the hippocampus when comparing severe AD to non-demented controls (39.8 +/- 11.8 vs 12.5 +/- 4.1 (PLA dots/cell), $p< 0.001$), moderate AD to controls (28.3 +/- 6.4 vs 12.5 +/- 4.1, $p<0.001$) or severe AD to moderate AD (39.8 +/- 11.8 vs 28.3 +/- 6.4 , $p<0.05$) (**Figure 2A, E**). In the dentate gyrus area, C99 levels were increased when comparing severe AD to non-demented controls (10.8 +/- 2.8 vs 2.5 +/- 1.1, $p<0.001$), moderate AD to non-demented controls (6.5 +/- 2.4 vs 2.5 +/- 1.1, $p<0.05$) and severe AD to moderate AD (10.8 +/- 2.8 vs 6.5 +/- 2.4) (**Figure 2B, E**). In the middle frontal gyrus of the frontal cortex, C99 levels were increased when comparing severe AD to controls (7.1 +/- 2.0 vs 2.3 +/- 1.6, $p<0.001$) and severe AD to moderate AD (7.1 +/- 2.0 vs 2.60 +/- 1.6, $p<0.001$) (**Figure 2C, E**). Levels of C99 in occipital cortex, an area considered to be resistant to neurodegeneration, were similar in all three groups (**Figure 2D, E**).

Co-staining with the neuronal nuclear marker Neu shows that C99 accumulates in the perinuclear region of neurons in non-demented subjects. Its distribution changes to an intranuclear pattern in Alzheimer's disease subjects (**Figure 3A**). Interestingly, C99 also accumulates in astrocytes in AD subjects, where it is localized in both the soma and processes, as revealed by GFAP staining. However, in contrast to neurons, the distribution of C99 in astrocytes does not change between non-demented and demented subjects (**Figure 3B**). Next, we compared the levels of beta-amyloid plaques and C99 in middle frontal cortex and occipital cortex. As seen in **Figure 4A,B**, Abeta

bioRxiv preprint doi: https://doi.org/10.1101/527572; this version posted January 22, 2019. The copyright holder for this preprint (which was not certified by peer review) is the author/funder. All rights reserved. No reuse allowed without permission.

plaques are present in both vulnerable and non-vulnerable areas, while C99 accumulation correlates with disease progression only in the middle frontal cortex, a vulnerable area, but not in the occipital cortex, a resistant area. These results show that C99 accumulation, as opposed to Abeta accumulation, is specific to neurons most vulnerable to neurodegeneration in Alzheimer's disease.

Discussion: Alzheimer's disease is characterized by accumulation of amyloid plaques and paired helical filaments. Mutations that cause early onset AD are located in the genes that code for the amyloid precursor protein, APP, and the enzyme responsible for amyloid production, Presenilin 1/Presenilin 2. These observations have led to the widely-held belief that beta-amyloid has a causative role in the development of AD. However, the distribution of amyloid deposits in the brain does not correlate well with disease progression. These results suggest the possibility that APP metabolites other than beta-amyloid might contribute to Alzheimer's disease. It has been proposed that C99, a specific APP metabolite, may cause neurodegeneration by inducing endosome enlargement (*12, 13*), leading to endosomal dysfunction and neuronal death (*14-17*).

In this study, we have developed a method to detect C99 *in situ*, and applied this method to measure the levels of C99 in postmortem human brain samples of individuals at different stages of Alzheimer's disease dementia. We found a correlation between levels of C99 and levels of cognitive decline in areas vulnerable to neurodegeneration, such as the hippocampus and frontal cortex. In the hippocampus, we found increased levels of C99 in the CA1 area and dentate gyrus in both moderate and severe AD, whereas in frontal cortex we found increased levels of C99 only in severe cases of AD, consistent with the well-established delayed involvement of frontal cortex in AD pathology. This correlation was absent in areas resistant to neurodegeneration, such as occipital cortex. In contrast to the area-specific increase in C99 levels, all areas studied in AD patients presented abundant amyloid plaques.

Using a new method to detect specific APP metabolites, we show that C99 accumulates selectively in vulnerable neurons, but not in resistant neurons, in the brains of Alzheimer's disease patients. Approaches to reduce amyloid burden, such as gamma-secretase inhibitors or immunotherapy, despite being successful at reducing beta-amyloid levels, have failed to stop or reduce the cognitive impairment that characterizes Alzheimer's disease. Semagacestat, a gamma-secretase inhibitor, worsened the symptoms of dementia in a large phase III clinical trial (*18*). It was speculated that

bioRxiv preprint doi: https://doi.org/10.1101/527572; this version posted January 22, 2019. The copyright holder for this preprint (which was not certified by peer review) is the author/funder. All rights reserved. No reuse allowed without permission.

this action may have been due to inhibiting the cleavage by gamma-secretase of other substrates such as Notch. We suggest here that the clinical failure may have been due, at least in part, to an accumulation of C99. Elucidation of the detailed molecular pathway that leads to the synthesis and breakdown of C99 is likely to reveal targets responsible for the regulation of this metabolite. Such information may greatly accelerate the development of therapeutic agents for the treatment of AD.

In conclusion, our results raise the possibility that C99, rather than Abeta, is responsible for the death of nerve cells in Alzheimer's disease. In that case, beta-secretase inhibitors, which lower both C99 and beta-amyloid are preferable to gamma-secretase inhibitors which lower beta-amyloid but increase C99 levels.

References

1. J. A. Hardy, G. A. Higgins, Alzheimer's disease: the amyloid cascade hypothesis. *Science* **256**, 184 (1992).
2. H. Braak, E. Braak, Staging of Alzheimer's disease-related neurofibrillary changes. *Neurobiology of aging* **16**, 271-278 (1995).
3. G. K. Gouras *et al.*, Intraneuronal Aβ42 accumulation in human brain. *The American journal of pathology* **156**, 15-20 (2000).
4. R. D. Terry *et al.*, Physical basis of cognitive alterations in Alzheimer's disease: synapse loss is the major correlate of cognitive impairment. *Annals of Neurology: Official Journal of the American Neurological Association and the Child Neurology Society* **30**, 572-580 (1991).
5. P. V. Arriagada, J. H. Growdon, E. T. Hedley-Whyte, B. T. Hyman, Neurofibrillary tangles but not senile plaques parallel duration and severity of Alzheimer's disease. *Neurology* **42**, 631-631 (1992).
6. R. L. Neve, N. K. Robakis, Alzheimer's disease: a re-examination of the amyloid hypothesis. *Trends in neurosciences* **21**, 15-19 (1998).
7. R. D. Terry, E. Masliah, L. A. Hansen, The neuropathology of Alzheimer disease and the structural basis of its cognitive alterations. *Alzheimer disease* **2**, 187-206 (1999).
8. P. T. Nelson *et al.*, Correlation of Alzheimer Disease Neuropathologic Changes With Cognitive Status: A Review of the Literature. *Journal of Neuropathology & Experimental Neurology* **71**, 362-381 (2012).
9. O. Söderberg *et al.*, Direct observation of individual endogenous protein complexes in situ by proximity ligation. *Nature methods* **3**, 995 (2006).
10. K. L. Youmans *et al.*, Intraneuronal Aβ detection in 5xFAD mice by a new Aβ-specific antibody. *Molecular neurodegeneration* **7**, 8 (2012).
11. C. Nordstedt, G. Caporaso, J. Thyberg, S. Gandy, P. Greengard, Identification of the Alzheimer beta/A4 amyloid precursor protein in clathrin-coated vesicles purified from PC12 cells. *Journal of Biological Chemistry* **268**, 608-612 (1993).

bioRxiv preprint doi: https://doi.org/10.1101/527572; this version posted January 22, 2019. The copyright holder for this preprint (which was not certified by peer review) is the author/funder. All rights reserved. No reuse allowed without permission.

12. Y. Jiang *et al.*, Alzheimer's-related endosome dysfunction in Down syndrome is Aβ-independent but requires APP and is reversed by BACE-1 inhibition. *Proceedings of the National Academy of Sciences* **107**, 1630-1635 (2010).
13. S. Kim *et al.*, Evidence that the rab5 effector APPL1 mediates APP-βCTF-induced dysfunction of endosomes in Down syndrome and Alzheimer's disease. *Molecular psychiatry* **21**, 707 (2016).
14. I. Lauritzen *et al.*, The β-secretase-derived C-terminal fragment of βAPP, C99, but not Aβ, is a key contributor to early intraneuronal lesions in triple-transgenic mouse hippocampus. *Journal of Neuroscience* **32**, 16243-16255 (2012).
15. I. Lauritzen *et al.*, Intraneuronal aggregation of the β-CTF fragment of APP (C99) induces Aβ-independent lysosomal-autophagic pathology. *Acta neuropathologica* **132**, 257-276 (2016).
16. A. Bourgeois *et al.*, Intraneuronal accumulation of C99 contributes to synaptic alterations, apathy-like behavior, and spatial learning deficits in 3ÕTgAD and 2ÕTgAD mice. *Neurobiology of aging* **71**, 21-31 (2018).
17. L.-W. Jin, I. Maezawa, I. Vincent, T. Bird, Intracellular accumulation of amyloidogenic fragments of amyloid-β precursor protein in neurons with Niemann-Pick type C defects is associated with endosomal abnormalities. *The American journal of pathology* **164**, 975-985 (2004).
18. R. S. Doody *et al.*, A phase 3 trial of semagacestat for treatment of Alzheimer's disease. *New England Journal of Medicine* **369**, 341-350 (2013).

Acknowledgments: We thank Dr. Fred Gorelick for discussion and Dr. Jean-Pierre Roussarie for providing reagents and discussion. We thank Alison North and the Bio-imaging facility at The Rockefeller University for training and advice in super-resolution microscopy. We thank Elisabeth Griggs for figure composition.

Funding: This work was supported by the Fisher Center for Alzheimer's Research Foundation, The Cure Alzheimer's fund and JPB Grant 794 (to P.G.). V.B. was supported by DOD/USAMRAA Grant W81XWH-14-1-0045.

Author contributions: M.P. performed the PLA experiments and confocal microscopy imaging. M.H. performed the super-resolution microscopy. V.H. contributed reagents and measured Abeta plaques. M.P., P.G. and V.B. analyzed data. M.P., P.G. and V.B. designed the project and wrote the manuscript.

Competing interests: Authors declare no competing interests.

Data and materials availability: All data are available in the main text or the supplementary materials.

bioRxiv preprint doi: https://doi.org/10.1101/527572; this version posted January 22, 2019. The copyright holder for this preprint (which was not certified by peer review) is the author/funder. All rights reserved. No reuse allowed without permission.

Methods

Antibodies

Primary antibodies used were anti-NeuN, Millipore; anti-GFAP, Abcam; anti-N-terminal C99, 6C3, Abcam, anti-Abeta 6E10, Covance, and RU-369 produced at the Rockefeller University. Secondary antibody was AlexaFluor 488 from Molecular Probes.

Proximity ligation assay (PLA) in cells

N2A cells stably overexpressing APP-695 were cultured in DMEM medium (Gibco, catalog number 11965-092), Opti-MEM (Gibco, catalog number 51985-034), supplemented with 5% FBS (Sigma, catalog number F4135), 100 ug/ml of Penicillin/Streptomycin (Gibco, catalog number 15140-122) and 500 ug/ml Geneticin (Gibco, catalog number 10131-027). Twenty thousand cells were seeded in 12 mm glass coverslips (Corning, catalog number 354085) in a12-well plate and allowed to attach for 24 hrs. Next, cells were incubated overnight with 5 uM BACE inhibitor IV (Millipore Sigma, catalog number 565788) or 1 uM gamma-secretase inhibitor L-685,458 (Sigma, catalog number L1790) or DMSO (Sigma, catalog number 276855) 0.1% as a control.

Next day, the cells were washed with PBS, fixed in 4% paraformaldehyde in PBS for 10 min at room temperature, permeabilized in PBST (PBS with 0.2 % Triton X-100) for 10 min, blocked in 10% goat serum in PBST and incubated in primary antibody overnight in blocking solution. Primary antibodies used to recognize C99 were: RU-369 (Immune serum raised in rabbit, 1:50 dilution) and 6C3 (Abcam, catalog number 126649 raised in mouse, 1:50 dilution). Next, the Duolink kit was used to develop the PLA signal (Sigma, catalog number DUO92008). Cells were then washed twice for 10 min each time in wash buffer A, incubated with PLA probe solution for 1 h at 37 °C, washed again in wash buffer A, and incubated in ligation-ligase solution for 30 min at 37 °C. Coverslips were washed in wash buffer A and incubated in amplification-polymerase solution for 100 min at 37 °C, washed twice for 10 min each time in wash buffer B. Next, the coverslips were mounted in duolink mounting media with DAPI. The specificity of the signal was controlled by omitting one of the antibodies. Cells were imaged using a Zeiss LSM710 laser confocal microscope. Quantification of PLA signal was performed using Image J software (NIH).

N2A cells stably overexpressing APP-695 were seeded on sterile, Zeiss high-performance cover glass at a density of 175,000 cells/well and grown overnight. Cells were treated with DMSO or a

bioRxiv preprint doi: https://doi.org/10.1101/527572; this version posted January 22, 2019. The copyright holder for this preprint (which was not certified by peer review) is the author/funder. All rights reserved. No reuse allowed without permission.

gamma secretase inhibitor (1 μM) in media for 3 hours. Cells were fixed with 4% PFA in PBS for 10 min at room temperature, permeabilized with PBST (PBS with 0.2 % Triton X-100) for 10 min at room temperature, and blocked in Duolink® PLA blocking solution for 1 hour at 37 °C. The cells were then incubated with primary antibodies RU-369 and 6C3, both at a 1:50 dilution in the Duolink® antibody diluent, overnight at 4°C. PLA was conducted the next day using the Duolink® PLA kit according to manufacturer's instructions until the mounting step in which the cells were separately stained for DAPI and then mounted onto a glass slide using VECTASHIELD® Antifade Mounting Medium without DAPI (Vector, catalog number H-1000). Coverslips were sealed with metallic nail polish and stored in the dark at 4°C until imaging. Super resolution three-dimensional images were taken using a DeltaVision OMX™ microscope in Structured Illumination mode. 568 nm and 405 nm lasers were used to image DAPI and PLA. Camera temperatures were kept at -80 °C, chamber temperature was kept at 23 °C, and an immersion oil with a refractive index of 1.515 was used. Z-stacks were taken to include all visible PLA dots and nuclei on the coverslip. The image data acquired by DeltaVision OMX was then reconstructed using softWoRx Imaging Workstation. Linespacing, best fit for K0, and amplitude values were evaluated to ensure the quality of the reconstruction. The reconstruction was then subjected to further processing by the "OMX Align Image" function. The final image was then compared to a widefield version of the same image using the "Generate Widefield" and "Deconvolve" functions on the raw non-reconstructed data. Individual sections from the total z-stack were used for comparison.

Proximity ligation assay in human brain sections.

Fifty-one human brain slides from hippocampus, frontal cortex and occipital cortex were obtained from the brain bank at Mount Sinai/JJ Peters VA Medical Center NIH Brain and Tissue Repository. Donors were selected to evidence no neuropathology, or only the neuropathology of AD excluding any other discernable neuropathology, such a cerebrovascular disease or Lewy bodies. Before proceeding with the staining protocol, the slides were deparaffinized and rehydrated. Incomplete removal of paraffin can cause poor staining of the section. Slides were placed in a rack, and the following washes were performed: 1. Xylene: 2 x 3 minutes. 2. Xylene 1:1 with 100% ethanol: 3 minutes 3. 100% ethanol: 2 x 3 minutes 4. 95% ethanol: 3 minutes 5. 70 % ethanol: 3 minutes 6. 50 % ethanol: 3 minutes. At the end of the washes, the brain slides were rinsed with water. Antigen

bioRxiv preprint doi: https://doi.org/10.1101/527572; this version posted January 22, 2019. The copyright holder for this preprint (which was not certified by peer review) is the author/funder. All rights reserved. No reuse allowed without permission.

retrieval was performed by microwaving the slides for 20 min in citric buffer. Next, the slides were permeabilized in PBST (PBS with 0.2 % Triton X-100) for 10 min, blocked in 10% goat serum in PBST and incubated in primary antibody overnight in blocking solution. Primary antibodies used to recognize C99 were: RU-369 (Immune serum raised in rabbit, 1:50 dilution) and 6C3 (Abcam, catalog number 126649 raised in mouse, 1:50 dilution). Next, the Duolink kit was used to develop the PLA signal (Sigma, catalog number DUO92008). Cells were then washed twice for 10 min each time in wash buffer A, incubated with PLA probe solution for 1 h at 37 °C, washed again in wash buffer A, and incubated in ligation-ligase solution for 30 min at 37 °C. Coverslips were washed in wash buffer A and incubated in amplification-polymerase solution for 100 min at 37 °C, washed twice for 10 min each time in wash buffer B. Next, the slides were incubated in 0.001% DAPI in wash buffer B for 5 min. Then, to quench autofluorescence, the slides were treated with "Trueblack" (Biotum, catalog number 23007) in 70% ethanol for 1 min. Then, the slides were mounted using Fluoromount G. Slides were imaged using a Zeiss LSM710 laser confocal microscope. For coimmunofluorescence of C99-PLA with neuron and astrocyte markers, primary antibodies were used together with PLA antibodies and secondary antibodies together with PLA probes.

PLA quantification.

C99-PLA produces bright red dots that were quantified using Image J software (NIH). The tiff images were thresholded, and the function "Analyze particles" was applied in the red channel. In the blue channel, corresponding to DAPI staining, the function "Cell counter" was applied after threshold.

OMX 3D-SIM using DeltaVision OMX

N2A695 cells were seeded on sterile, Zeiss high-performance cover glass at a density of 175,000 cells/well and grown overnight. Cells were treated with DMSO or a gamma secretase inhibitor (1 μM) in media for 3 hours. Cells were fixed with 4% PFA in PBS and then permeabilized with 0.2% PBS-Triton. Cells were blocked for one hour in Duolink® PLA blocking solution at 37°C. The cells were then incubated with primary antibodies APP369 and C99, both at a 1:50 dilution in the Duolink® antibody diluent, overnight at 4°C. PLA was conducted the next day using the Duolink® PLA kit according to the manufacturer's instructions until the mounting step in which the cells were separately stained for DAPI and then mounted onto a glass slide using

bioRxiv preprint doi: https://doi.org/10.1101/527572; this version posted January 22, 2019. The copyright holder for this preprint (which was not certified by peer review) is the author/funder. All rights reserved. No reuse allowed without permission.

VECTASHIELD® Antifade Mounting Medium without DAPI. Coverslips were sealed with metallic nail polish and stored in the dark at 4°C until imaging. Super resolution three-dimensional images were taken using a DeltaVision OMX™ microscope in Structured Illumination mode. 568 nm and 405 nm lasers were used to image DAPI and PLA. Camera temperatures were kept at -80°, chamber temperature was kept at 23°C, and an immersion oil with a refractive index of 1.515 was used. Z-stacks were taken to include all visible PLA dots and nuclei on the coverslip. The image data acquired by DeltaVision OMX was then reconstructed using softWoRx Imaging Workstation. Linespacing, best fit for K0, and amplitude values were evaluated to ensure the quality of the reconstruction. The reconstruction was then subjected to further processing by the OMX Align Image function. The final image was then compared to a widefield version of the same image using the generate widefield and deconvolve functions on the raw non-reconstructed data. Individual sections from the total z-stack were used for comparisons.

Amyloid plaque staining

Sections from paraffin-embedded blocks were stained using hematoxylin-eosin and anti–β amyloid 4G8 and anti-tau AD2. All neuropathological data regarding the extent and distribution of neuropathological lesions were collected by neuropathologists unaware of any of the clinical and psychometric data.

For quantitative measures of plaque density, 5 representative high-power fields (0.5 mm^2) were examined and an average density score was calculated for each region and expressed as mean plaque density per square millimeter. When plaques were unevenly distributed in each slide, plaques in the region with the highest density were counted.

Statistical analysis

The data are presented as means ± SD. The significance level was determined using a two-way ANOVA with Bonferroni post-test, comparing severe versus non-demented control, moderate versus non-demented control and severe versus moderate. Correlations were calculated using Pearson product moment correlations. All statistical analyses were performed by using GraphPad Prism software.

bioRxiv preprint doi: https://doi.org/10.1101/527572; this version posted January 22, 2019. The copyright holder for this preprint (which was not certified by peer review) is the author/funder. All rights reserved. No reuse allowed without permission.

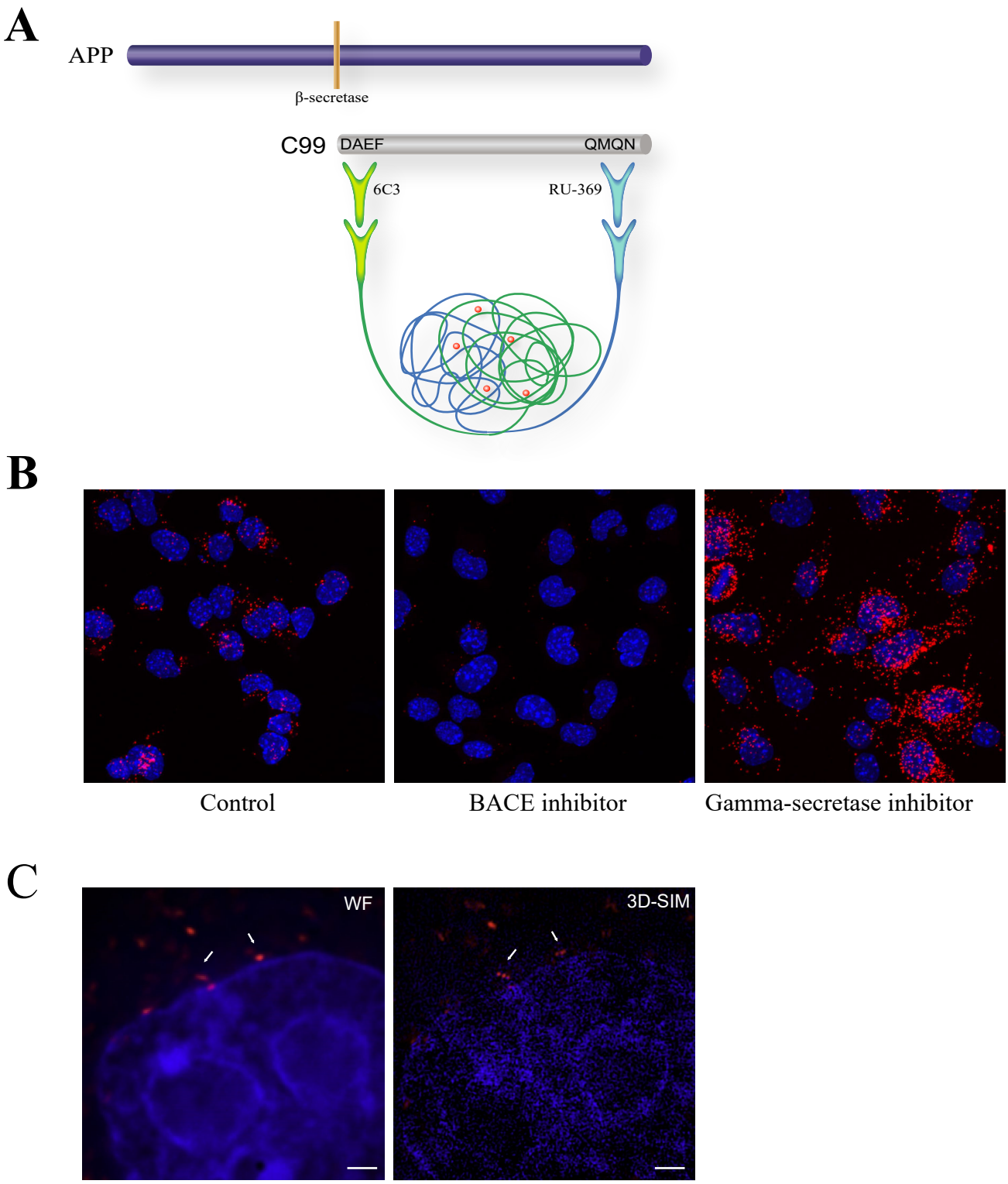

Figure 1. Adaptation of the proximity ligation assay (PLA) for quantitative analysis of C99. A) Diagram showing the location of epitopes for the antibodies (6C3 and RU-369) used in this PLA. B) N2A cells overexpressing APP695 in control conditions (left panel), with BACE inhibitor (middle panel), or with gamma-secretase inhibitor (right panel). Nuclear marker DAPI is in blue and PLA signal is in red. C) Super-resolution microscopy, in wide field (WF, left) and after 3D reconstruction (right), showing that each dot as seen by wide field corresponds to a collection of 2-3 smaller dots (arrows). Scale bar: 1 uM.

bioRxiv preprint doi: https://doi.org/10.1101/527572; this version posted January 22, 2019. The copyright holder for this preprint (which was not certified by peer review) is the author/funder. All rights reserved. No reuse allowed without permission.

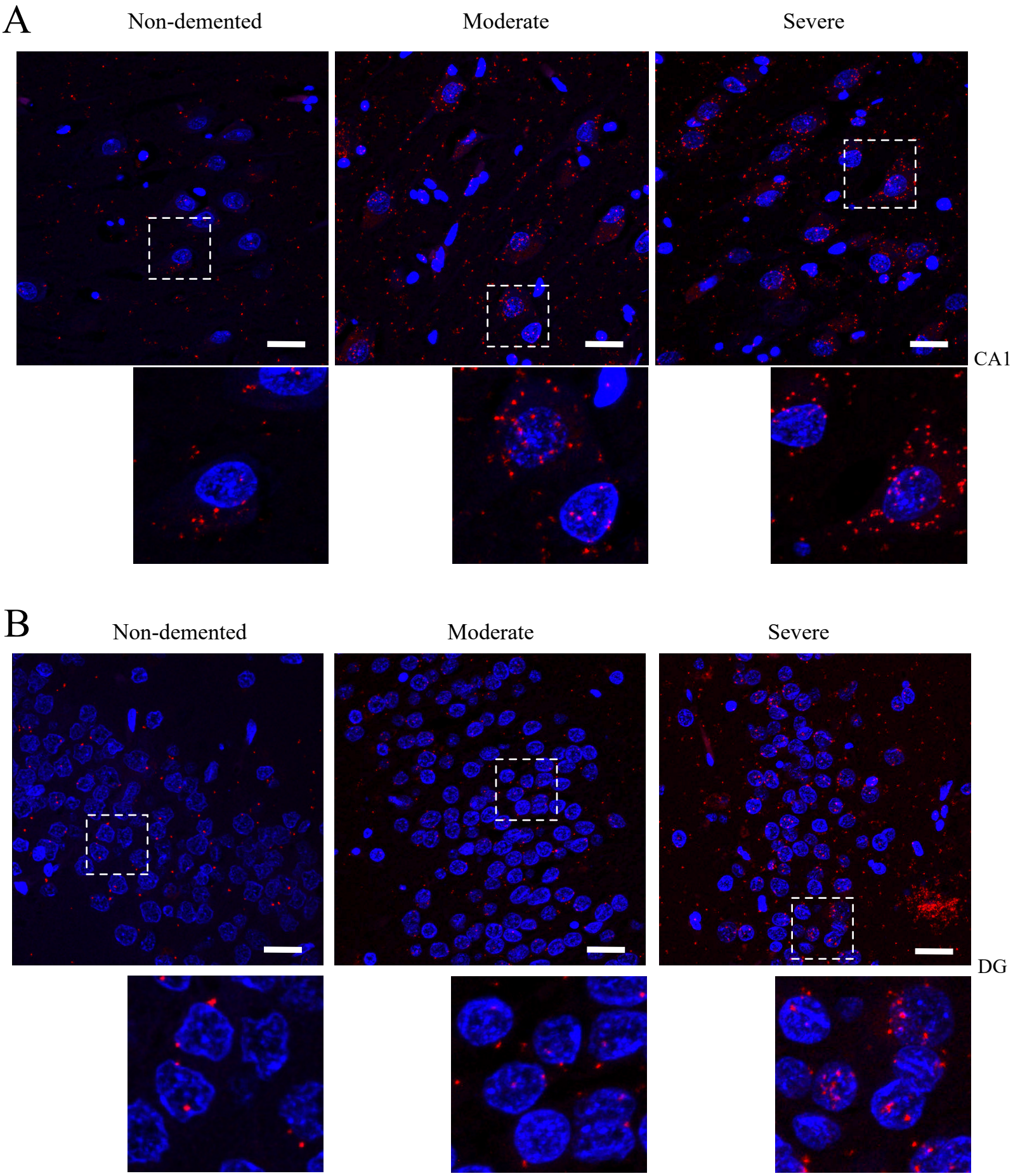

Figure 2. Continue

bioRxiv preprint doi: https://doi.org/10.1101/527572; this version posted January 22, 2019. The copyright holder for this preprint (which was not certified by peer review) is the author/funder. All rights reserved. No reuse allowed without permission.

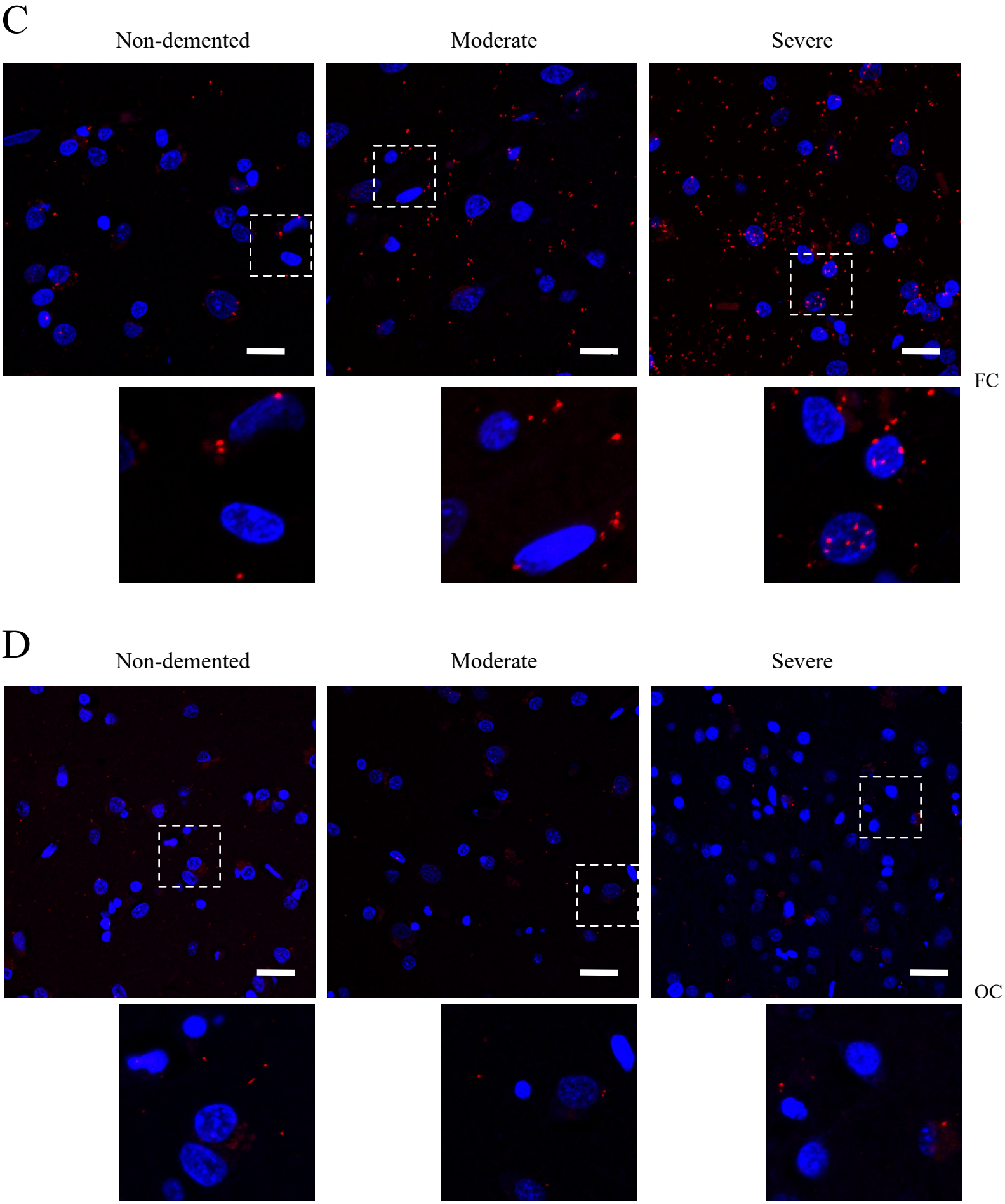

Figure 2. Continue

bioRxiv preprint doi: https://doi.org/10.1101/527572; this version posted January 22, 2019. The copyright holder for this preprint (which was not certified by peer review) is the author/funder. All rights reserved. No reuse allowed without permission.

E

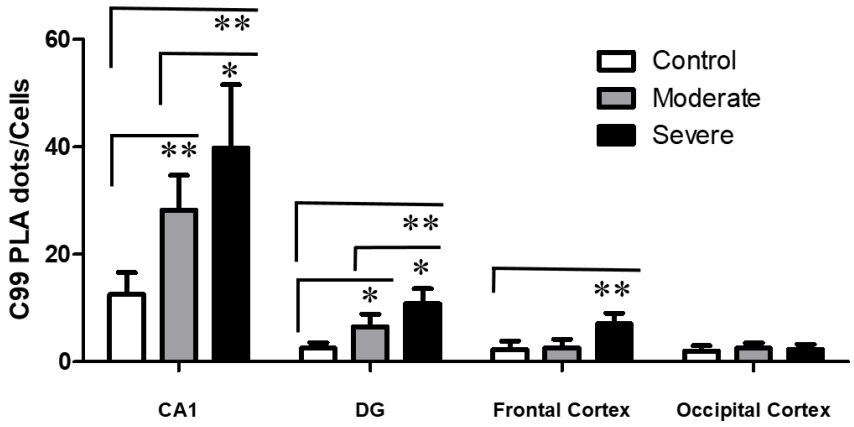

Figure 2. Elevated levels of C99 in vulnerable neurons from brains of AD patients as measured by PLA. Representative images of C99 in A) CA1, B) dentate gyrus (DG), C) frontal cortex (FC) and D) occipital cortex (OC) from moderate and severe Alzheimer's disease patients and non-demented control subjects. PLA is in red and DAPI in blue. Scale bar: 20 um. E) Quantification of C99 levels in CA1, DG, FC and OC of control, moderate and severe Alzheimer's disease brains. Data represent means ± SD.* $P<0.05$, * $P<0.01$, ANOVA two way with Bonferroni post-test.

bioRxiv preprint doi: https://doi.org/10.1101/527572; this version posted January 22, 2019. The copyright holder for this preprint (which was not certified by peer review) is the author/funder. All rights reserved. No reuse allowed without permission.

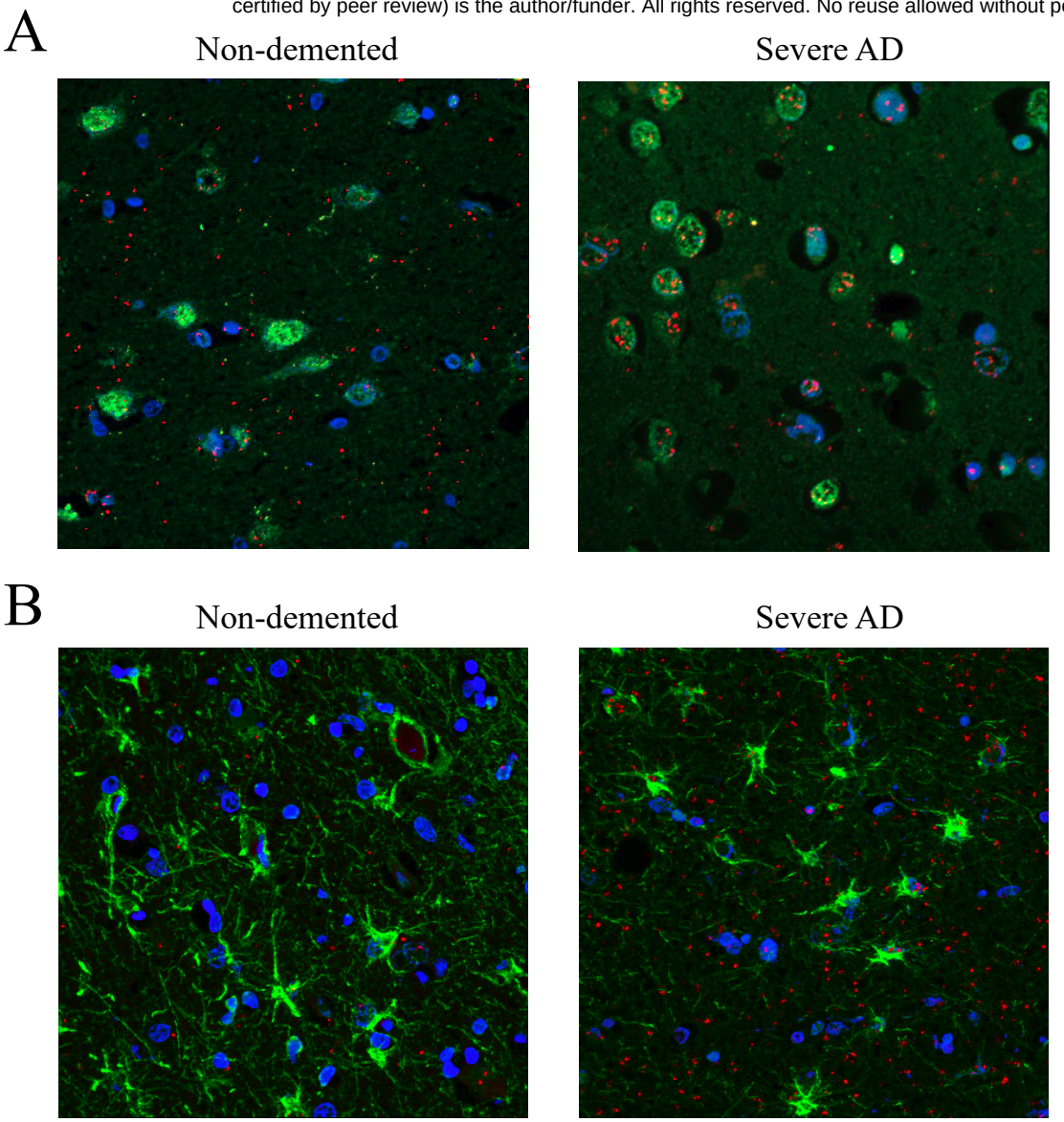

Figure 3. Aberrant localization of C99 in vulnerable neurons in AD. A) C99 distribution in neurons from a non-demented control subject (left panel) compared to a severe case of AD (right panel). Note the colocalization of C99 with NeuN in the nucleus of vulnerable neurons in AD. PLA is in red, NeuN is in green and DAPI in blue. B) C99 distribution in astrocytes from a non-demented control subject (left panel) compared to a severe case of AD (right panel). PLA is in red, GFAP is in green and DAPI in blue.

bioRxiv preprint doi: https://doi.org/10.1101/527572; this version posted January 22, 2019. The copyright holder for this preprint (which was not certified by peer review) is the author/funder. All rights reserved. No reuse allowed without permission.

A

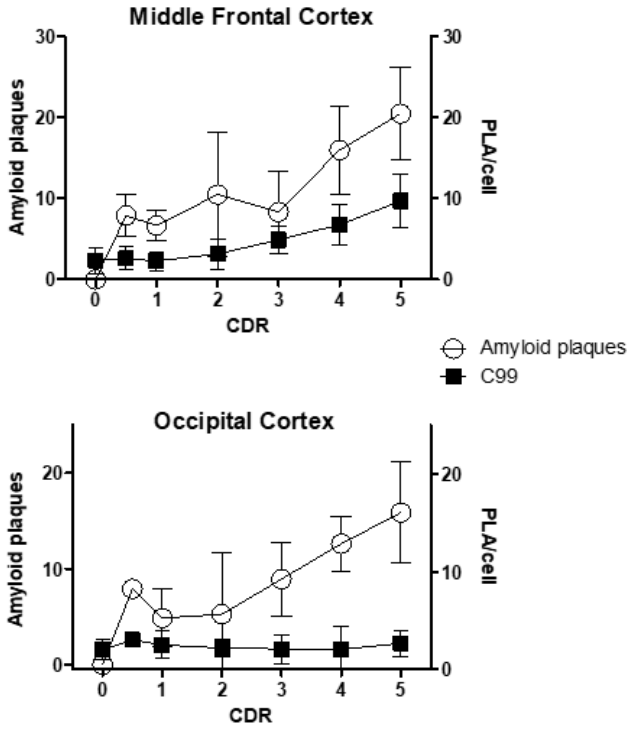

B

	Middle Frontal Cortex	
	beta-amyloid	C99
Pearson r	0.91	0.95
P value (two tailed)	0.0035	0.0011

	Occipital Cortex	
	beta-amyloid	C99
Pearson r	0.90	-0.08
P value (two tailed)	0.0052	0.856

Figure 4. C99 correlates better than beta-amyloid with vulnerability to AD. A) Correlation between cognitive decline and beta-amyloid or C99 levels in the middle frontal cortex (upper graph) or the occipital cortex (lower graph). B) Statistical analysis of the correlation, two-tailed Pearson correlation.